International Journal of Mass Spectrometry 299 (2011) 131–138

Contents lists available at ScienceDirect

International Journal of Mass Spectrometry

journal homepage: www.elsevier.com/locate/ijms

"Ion surfing" with radiofrequency carpets

G. Bollen

Michigan State University, National Superconducting Cyclotron Laboratory, 1 Cyclotron, East Lansing, MI 48824, USA

ARTICLE INFO

Article history:
Received 12 July 2010
Received in revised form
18 September 2010
Accepted 30 September 2010
Available online 20 October 2010

Keywords:
Ion transport
Carpet
Radiofrequency
Beam stopping

ABSTRACT

The transport of low-energy ions by inhomogeneous alternating electric fields combined with static electric fields is an important and established technique in applied and fundamental research. Radiofrequency (RF) multipole ion guides can focus and transport ions along a linear path while RF funnels, carpets, or walls provide ion guiding along surfaces. A novel surface transport technique – ion surfing – is proposed which relies on a traveling potential wave combined with a static repelling RF field. The results of numerical simulations are presented and the observed features of ion surfing are discussed. In addition, possible applications to thermalized (gas-stopped) fast ion beams are presented.

1. Introduction

The confinement and transport of low-energy ions by means of time-dependent, alternating-gradient focusing is a powerful and widely applied technique. Devices most commonly used are linear radiofrequency (RF) multipole ion guides to transport ions along a line path. Operated in the presence of a light buffer gas, these devices can act as beam coolers. Ion guiding and cooling is applied in ion chemistry as well as atomic and molecular physics. It is also applied in nuclear physics for the preparation of high-quality, low-energy rare isotopes beams [1–5]. In addition to ion transport along a line path there are situations in which transport over surfaces is required. This is of particular importance for stopping and thermalizing of energetic (MeV–GeV) rare isotopes produced by nuclear reactions or as recoils from nuclear decay [6–14]. In so-called gas stoppers or gas catchers fast multi-charged ions are initially slowed down in matter and finally stopped in a chamber filled with helium gas. Since they remain singly or doubly-charged in ultra-pure helium [15] they can be guided to an extraction orifice. After leaving the stopping chamber linear RF multipole ion guides are usually employed to guide the ions into high-vacuum where they are accelerated to form a low-emittance low-energy beam. In present gas stopper systems for rare isotopes ion transport is either obtained by static electric fields combined with gas flow or by gas flow combined with static and RF fields, created by electrode geometries named RF funnels, RF carpets, or RF walls [6,16]. The common feature of all devices that involve RF for ion transport along surfaces is the use of a series of parallel or concentric electrodes to which RF voltages are applied with a 180° phase difference between adjacent electrodes. The resulting time-dependent alternating electric field gradient provides a time-averaged force that repels the ion. In addition, static voltages are usually superimposed to the electrodes to create a potential gradient along the surface that guides the ions parallel to surface.

The application of the present surface transport techniques to large systems is challenging. For transport over long distances a large number of static voltages are needed to produce a voltage gradient. These static voltages must be combined with the opposite-phase RF voltages applied to the electrodes. Present solutions use in-vacuum resistor chains or a large number of vacuum feedthroughs to bring the voltages to the individual electrodes. The electrode pitch is typically below 1 mm and values as small as 0.2 mm are used [6]. A corresponding large number of voltages must be generated, hundreds and more in the case of transport over distances as large as 1–2 m. In addition, the maximum achievable potential gradient is limited by high voltage breakdown in the helium gas and also by the competing effective force of the RF carpet and the guiding dc field. Depending on the gas pressure and the geometry of the system, typical maximum voltages are of the order of one kilovolt. This limits the typical potential gradient, which determines the transport velocity, to values of the order of 10 V/cm.

In this paper, an alternative concept is discussed for ion transport along surfaces using a traveling potential wave instead of a static electric potential gradient combined with a repelling RF field. It should be noted that this approach has many aspects in common with pioneering work performed by S. Masuda and coworkers in the Seventies on the transport of charged, macroscopic particles in

E-mail addresses: bollen@frib.msu.edu, bollen@nscl.msu.edu

1387-3806/$ – see front matter © 2010 Elsevier B.V. All rights reserved.
doi:10.1016/j.ijms.2010.09.032

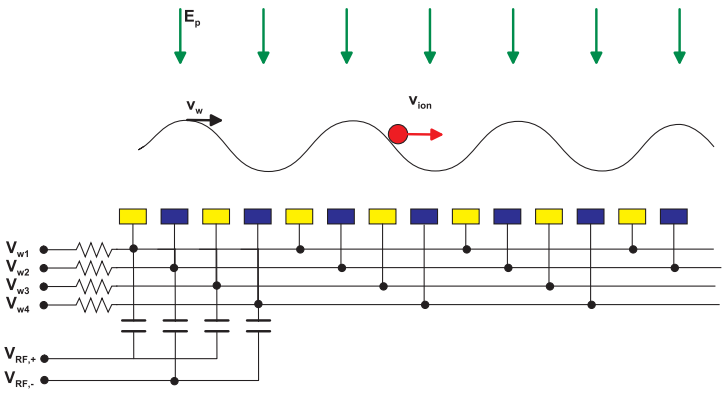

Fig. 1. Schematic for a radiofrequency (RF) carpet and its operation in "ion surfing" mode. In addition to the RF voltages $V_{RF,\pm}$ to create a repelling force, high-frequency (HF) voltages $V_{w,i}$, $i = 1, 4$ are applied to create a traveling surface wave with wave velocity v_w. A static electric field with strength E_p pushes the ions towards the carpet.

air or liquids by means of traveling potential waves [17–19]. One important difference of the "ion surfing" mode developed in this work is the combination of a static repelling RF field with a traveling potential wave. This leads to new transport features not achievable with traveling waves only. The ion surfing mode promises faster and easier ion transport over long distances in gas stoppers, lower maximum voltages and a simpler circuitry than schemes presently in use.

2. Concept of ion surfing on RF carpets

Fig. 1 illustrates the general principle of the ion surfing transport. A static pushing field with strength E_p guides the ions towards an RF carpet surface. Close to the surface, the resulting force is counteracted by a repelling effective potential, created by RF voltages $V_{RF,\pm}$ applied to the carpet electrodes as in usual RF carpets. An effective potential minimum is formed where ions will accumulate due to damping by gas collisions. Now, in order to move the ions parallel to the surface, phase-shifted high-frequency (HF) voltages $V_{w,i}$, $i = 1, N$ are applied to create a traveling potential wave with wave velocity v_w. For the case illustrated in the figure, a wavelength of 4 times the electrode pitch is used. Fig. 1 provides an overview of the effective potential experienced by the ions and its main contributions. Two different transport modes can be expected in the ion surfing scheme

- The ion is "locked" to the traveling potential wave and moves with a velocity equal to the wave velocity, $v_i = v_w$.
- The ion motion is not locked but the ion is dragged by the potential wave, "slipping" over the crests, resulting in ion velocities $v_i < v_w$.

Before demonstrating that these two modes exist, the forces seen by the ion are discussed in the following section.

2.1. Damping

The gas stoppers and beam coolers mentioned above always contain light buffer gas. The damping of the ion motion by many individual collisions with the buffer gas atoms can be fully taken into account in calculations of ion trajectories. However, when the collision rate is very large it is often sufficient to describe the overall effect by an average damping force [20]. For low ion velocities $\vec{v}$ a viscous force provides a good description of the damping:

$$\vec{F}_d = -D \cdot \vec{v}, \tag{1}$$

The damping factor $D = q/m/K$ is determined by the ion mobility K [21], which is itself inversely proportional to the pressure p and proportional to the temperature of the gas, and by the ion's charge q and mass m.

2.2. Pushing and repelling force

The ion surfing method requires that the ions are delivered to and kept close to the RF carpet in order for them to experience the traveling potential wave. A constant electric field $\vec{E}_p$ perpendicular to the carpet surface will be assumed in the present study.

The repelling force of the RF carpet is achieved by applying RF voltages to a series of parallel or concentric electrodes, with a 180° phase shift between neighboring electrodes and with an amplitude V_{RF} and a frequency ω_{RF}

$$V_{RF,\pm} = \pm V_{RF} \cdot \cos(\omega_{RF} t). \tag{2}$$

While the resulting potential as a function of distance from the carpet cannot be obtained analytically, an analytical expression for the electric field $\vec{E}_{RF}(x, y) = (E_x, E_y)$ was recently derived [22]. This expression is a very good approximation of present ion transport systems that use a series of parallel electrodes on a surface. The electric field for an electrode system with pitch a and gap g and ratio $\gamma = g/a$ is given by:

$$E_x = \frac{2V_{RF}}{\gamma a \pi}\left[\arctan\left(\frac{\sin(\pi[x/a+\gamma/2])}{\sinh(\pi\gamma/a)}\right) - \arctan\left(\frac{\sin(\pi[x/a-\gamma/2])}{\sinh(\pi\gamma/a)}\right)\right], \tag{3}$$

$$E_y = \frac{V_{RF}}{\gamma a \pi} \ln\left(\frac{\cosh(\pi y/a) + \cos(\pi[x/a+y/2])/\cosh(\pi y/a) - \cos(\pi[x/a+y/2])}{\cosh(\pi y/a) + \cos(\pi[x/a-y/2])/\cosh(\pi y/a) - \cos(\pi[x/a-y/2])}\right). \tag{4}$$

Here, x denotes the direction parallel to the surface and perpendicular to the electrode strips and y the direction normal to the surface. Compared to [22] the origin in Eq. (4) is shifted by $a/2$ in the x direction. The electric field expressions given above have been implemented in a code developed for the simulations performed in this work.

For distances $y > a$ these field expressions can be used to determine the effective average force. This force can be thought to originate from a pseudo potential [23] of the form:

$$V_{eff} = \frac{e}{4m\omega_{RF}^2}(E_x^2 + E_y^2), \tag{5}$$

If damping with a damping factor D is present, the pseudo potential will be reduced [6] by the damping to

$$V_{eff,d} = \frac{\omega_{RF}^2}{\omega_{RF}^2 + D^2} V_{eff}, \tag{6}$$

For distances $y > a$ the pseudo potential decreases approximately exponentially with the distance from the surface

$$V_{eff}(y) = V_{eff,max} \cdot e^{-2\pi(y/a)}. \tag{7}$$

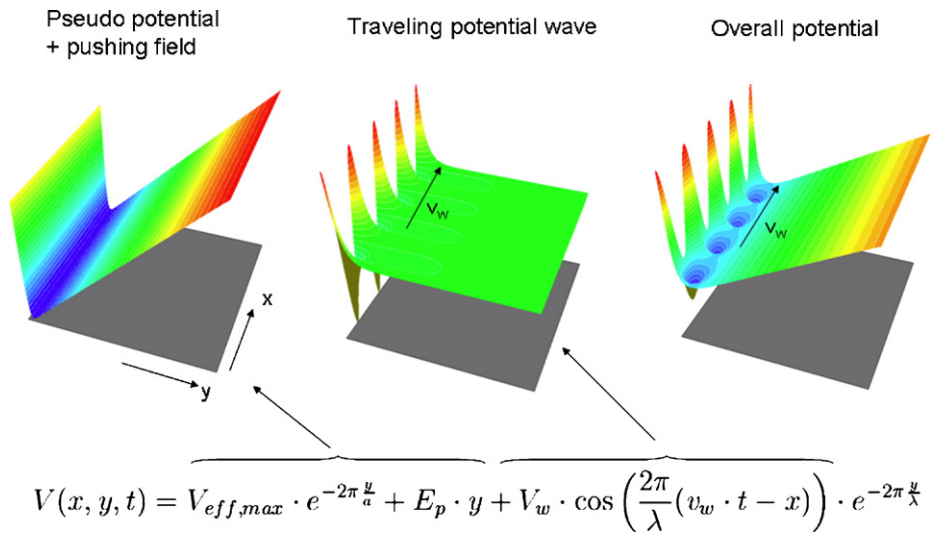

Fig. 2. Overall effective potential experienced by the ion during ion surfing.

This repelling potential together with the opposing pushing field results in an overall effective potential with a minimum parallel to the carpet surface as depicted in Fig. 2 (left). While the figure illustrates the situation in the case of ion surfing quite well, it should be noted that the underlying pseudo potential concept does not consider any loss of the ions that can occur if the strength and frequency of the alternating focusing–defocusing forces are outside the parameter space for stable motion.

2.3. Traveling potential wave

The traveling potential wave that is generated to move the ions parallel to the carpet surface by applying HF voltages of the form:

$$V_{w,i} = V_w \cdot \cos\left(\omega_w \cdot t + 2\pi\frac{i}{N} + \phi_w\right), \tag{8}$$

to groups of N electrodes, as shown in Fig. 1. These HF voltages have an amplitude V_w and are phase shifted by $2\pi/N$ from one electrode to the next. The wave length is given by

$$\lambda = N \cdot a. \tag{9}$$

Using a HF frequency ω_w results in a wave velocity of

$$v_w = \frac{1}{2\pi}\omega_w \cdot \lambda = \frac{Na}{2\pi}\omega_w. \tag{10}$$

Assuming a sinusoidal variation on the potential surface, the amplitude of the potential wave decreases exponentially with distance y from the surface,

$$V_w(x,y) = V_w \cdot \cos\left(\frac{2\pi}{\lambda}(v_w \cdot t - x)\right) \cdot e^{-2\pi(y/\lambda)}, \tag{11}$$

similar to that of the pseudo potential. Fig. 2 illustrates how the effective potential discussed above and the potential of the traveling wave add up to the overall potential experienced by the ion.

3. Ion surfing simulations

In order to demonstrate the ion surfing concept and to illustrate some of its features numerical simulations have been performed with two simulations codes. A dedicated fast code, IONSURF, was written to efficiently explore the parameter space for this technique. The analytical expressions as given by Eqs. (3) and (4) for the RF carpet field, Eq. (1) for the damping, and Eq. (11) for the traveling wave were used to describe the forces acting on the ion. Given these forces the IONSURF code uses a Runge-Kutta algorithm to numerically integrate the equation of motion of an ion. In order to benchmark the IONSURF code and validate the approximations made in the equations, simulations were also performed with the well-known SIMION code [24]. Planar electrode geometries similar to that illustrated in Fig. 1 were used and a SIMION user program was written for applying the RF voltages to the electrodes as described by Eqs. (2) and (8). The effect of the buffer gas collisions was taken into account by using a viscous damping force but a few calculation were performed using a hard-sphere collision model. A set of standard parameters used in the numerical simulations is given in Table 1.

3.1. Basic features of ion surfing

Fig. 3 shows an ion trajectory calculated with the SIMION code for the parameters given in Table 1. The pushing field was realized with a biased planar electrode mounted above the carpet. A negatively biased ion collection electrode was used to terminate the trajectory of the ion. The trajectory illustrates that the ion is first pushed towards the carpet and then transported parallel close to the surface. Near the carpet the ion is found to move with an average speed v_i equal to the velocity v_w of the applied potential wave.

Fig. 4 shows sample trajectories for a range of wave voltages U_w. Notice that at $U_w = 40$ V a locked motion with $v_i < v_w$ is observed soon after the ion is started. If the wave voltage is reduced below $U_w = 40$ V the forward pushing force is not strong enough to com-

Table 1
Set of standard parameters used in the computational study of ion surfing.

Parameter	Value
Ion mass number	100
Ion charge	1e
Electrode pitch	0.5 mm
Electrode gap-to-pitch ratio	0.7
RF frequency	4 MHz
RF amplitude U_{RF}	150 V
Wave velocity v_w	400 m/s
Wave amplitude U_w	40 V
Wave length λ	5 mm
Push field strength E_p	10 V/cm
Helium gas pressure p_{He}	100 mbar

pensate for the viscous drag force and the ion loses its lock with the traveling potential wave but it periodically falls back into a subsequent valley of the traveling wave. This "slipping mode" leads to a reduced transport velocity $v_i < v_w$ that becomes more pronounced as U_w is reduced. For voltages $U_w = 50$ V the force pointing towards the carpet eventually becomes strong enough to cause the ion to strike one of the carpet electrodes. In the bottom of the figure two ion trajectories are shown that have been calculated using a hard-sphere collision model instead of the simple viscous drag force employed in the calculations shown above. Good agreement of the characteristics of the ion trajectory is observed between the two different simulations, validating use of the more efficient viscous drag force in the numerical simulations.

3.2. Exploring the parameter space of ion surfing

The IONSURF code was used to explore the transport properties of ion surfing in greater detail. Two-dimensional scans of the wave velocity and the wave amplitude were performed. The ions were started at a distance $y = 2a$ above the carpet and trajectories were followed for one millisecond to obtain the values for the desired observables.

Fig. 5 shows contours of the average ion transport velocity v_i as a function of U_w and v_w. Ions will be transported in the parameter space that corresponds to the colored area and they are lost in the white area. A triangular region centered on $U_w = 40$ V is clearly identifiable in which the ion transport speed and the wave speed are the same, $v_i = v_w$. The figure shows that in this "locking mode" transport velocities as high as $v_i = 700$ m/s can be reached. In the remaining parameter space $v_i < v_w$ is observed. It is worth noting that in this "slipping mode" ion transport velocities well above 100 m/s can still be obtained.

Fig. 6 shows the velocity ratio v_i/v_w for different RF frequencies. The top figure has been calculated for $v_{RF} = 4$ MHz. The areas for "locking mode" (velocity ratio close to unity) and "slipping mode" (velocity ratio <1) are clearly distinguishable. The positions for the sample SIMION trajectory calculations shown in Fig. 4 are indicated by circles. Comparison of the trajectory features (locking, slipping, ion lost) again shows very good agreement between SIMION and IONSURF results. The bottom figure shows the result from calculations with $v_{RF} = 2$ MHz. It illustrates that lower RF frequencies lead to a reduction of the range of wave voltages for which transport can be maintained.

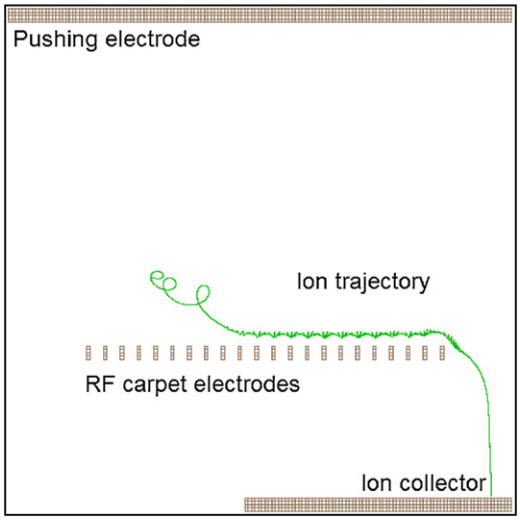

Fig. 3. Electrode configuration as used in SIMION for the ion transport simulations. The pushing electrode is positively biased to provide a field of about 10 V/cm in the gap above the carpet. The ion collector is biased negatively with respect to the carpet. The ion trajectory shown has been calculated with the parameters given in Table 1.

Given these very encouraging results, an interesting question that remains is how closely the ions approach the carpet surface? Fig. 7 shows the ratio of the minimum distance from the carpet surface to the electrode pitch y_{min}/a of the ion during its trajectory. Minimum distances larger than 10% of the electrode pitch are obtained for a very large fraction of the parameter space for which ion transport is possible. Distances increase as one moves towards and into "slipping mode".

Additional calculations were performed with the IONSURF code to study the effect of different push fields or ion masses. The ion surfing approach was found to be quite robust with respect to such changes. Fig. 8 shows simulation results for the parameters as listed in Table 1 but the push field strength E_p being increased from

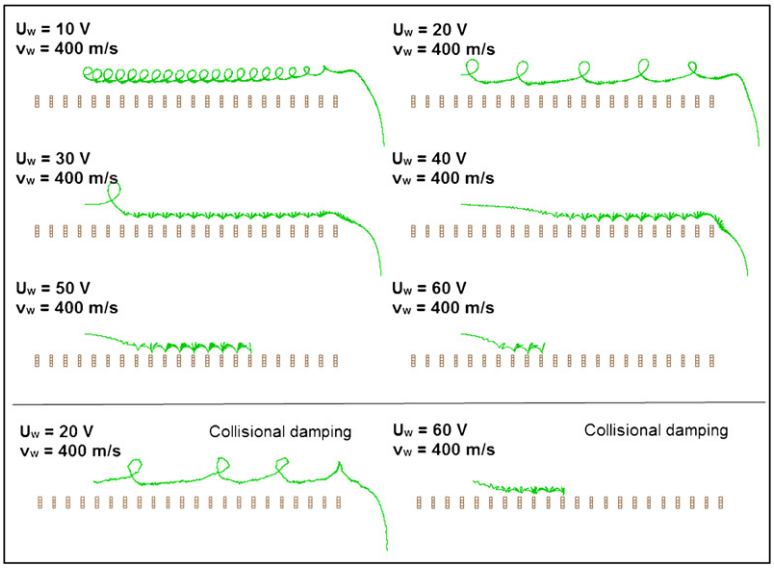

Fig. 4. Ion trajectories calculated with the SIMION code for different voltage amplitudes V_w of the traveling wave. The remaining parameters are given in Table 1. Top rows: results of calculations in which the damping effect of the helium ion interaction is described by a simple drag force. Bottom row: trajectories obtained with a hard-sphere collision model to describe the helium-ion interaction.

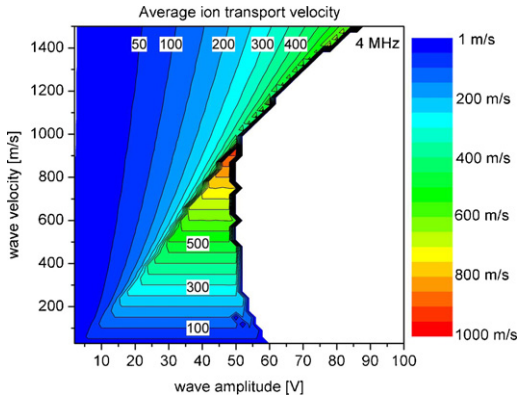

Fig. 5. Contours of the average ion transport velocities v_i calculated with the ION-SURF code as a function of wave voltage U_w and wave velocity v_w.

10 V/cm to 50 V/cm and to 200 V/cm. The overall transport features are maintained but a stronger push field reduces the maximum wave amplitude U_W for which successful transport is observed.

All RF transport techniques (RF quadrupole ion guides, RF carpets and funnels) show a mass dependence of the parameter space in which ion transport is possible. This is also the case for ion surfing as illustrated in Fig. 9. The parameters given in Table 1 have been used for ions with mass numbers $A = 50$ and $A = 150$. The results show that ions with heavier masses are transported for a larger range of wave amplitudes U_W. For lighter masses this range is reduced but can be recovered to some extent by increasing the

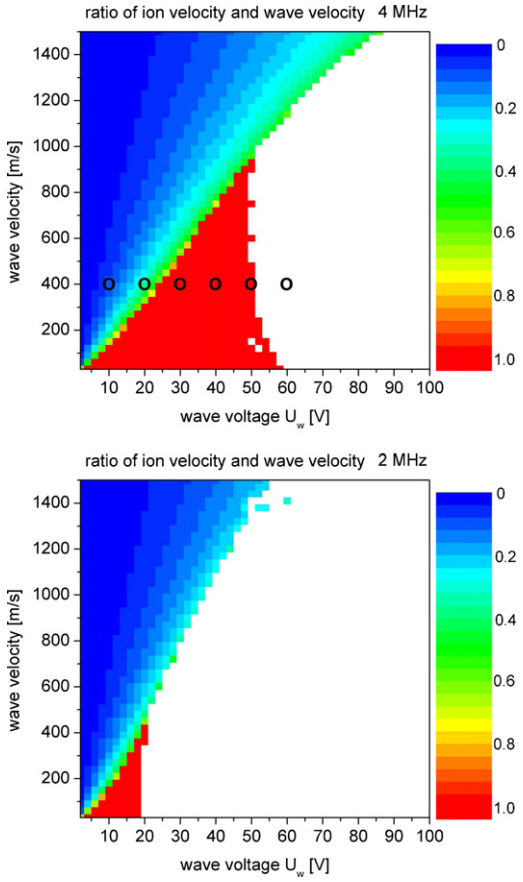

Fig. 6. Ratio of ion transport velocity and wave velocity calculated with the ION-SURF code as a function of wave voltage U_w and wave velocity v_w for RF frequencies $v_{RF} = 4$ MHz (top) and $v_{RF} = 2$ MHz (bottom) applied to the carpet. The circles indicate the parameter values used for the SIMION calculations shown in Fig. 4.

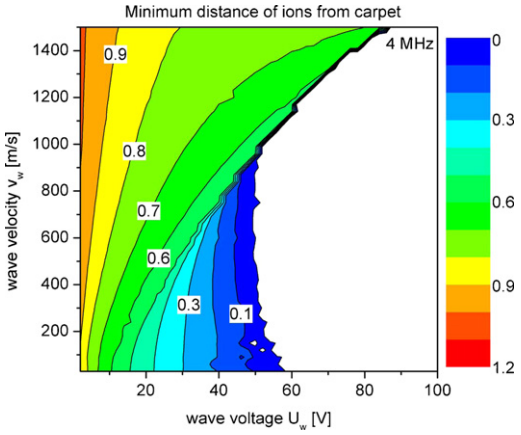

Fig. 7. Minimum distance of the ion trajectories y_{min} above the carpet surface, measured in units of the electrode pitch a of the carpet.

RF frequency as demonstrated in the figure for the case of $A = 50$ ions.

3.3. Ion squeezing: a variant of ion surfing

In the context of this study a variant of the ion surfing method was briefly investigated with the SIMION code and further studies are underway. Two parallel RF carpets are brought close to each other and potential waves are applied to both of them with the same wave velocity and phase. No pushing field would be applied. It should be noted that this concept is the same as one of those used by Masuda on the movement of blood cells in liquid by traveling waves [19]. It is also similar to transport of ions by traveling pulses demonstrated in a stacked-ring ion guide [25].

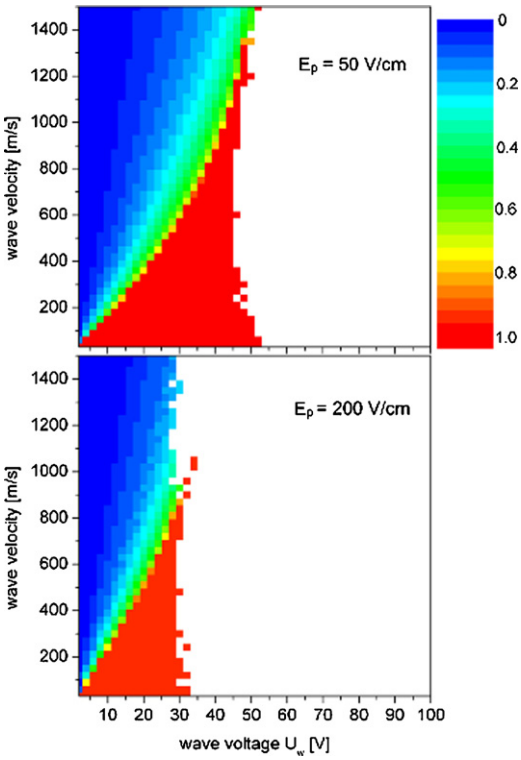

Fig. 8. Ratio of ion transport velocity and wave velocity as a function of wave voltage U_w and wave velocity v_w for a push field $E_p = 50$ V/cm (top) and $E_p = 200$ V/cm (bottom).

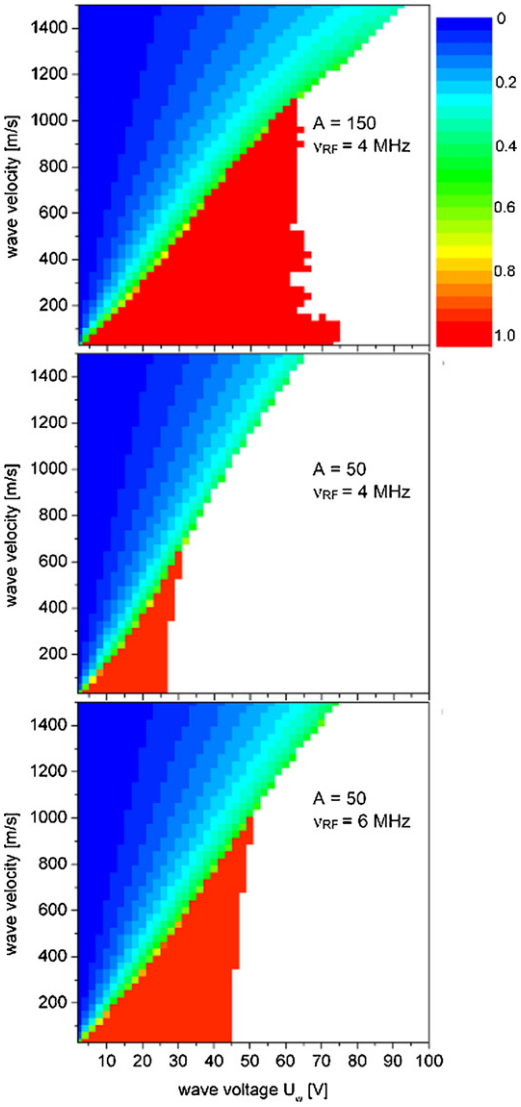

Fig. 9. Ratio of ion transport velocity and wave velocity as a function of wave voltage U_w and wave velocity v_w for an ion with mass number $A = 150$ (top) and for $A = 50$ (middle and bottom). RF frequencies ν_{RF} of 4 MHz and 6 MHz are used for the $A = 50$ calculations.

For the parallel RF carpet system discussed here ion transport can be expected to work best if the distance between both carpets is of the order of the wavelength of the traveling wave. Under such conditions the effect of a pushing field would be provided by the potential waves themselves and depending on the chosen parameters the ions would either move in locked or in slipping mode in the space between the two carpets.

Fig. 10 demonstrates "ion squeezing" of ions through such a systems and for the RF amplitudes used locked (top) and slipping motion (bottom) is observed. In the locked mode ions are transported close to one of the carpets (moved by the potential buckets visible in Fig. 2) while in the slipping mode the traveling waves push them to the midplane between both carpets.

It is apparent that such a scheme can easily be expanded to provide a larger volume in which ions can be stopped and transported. For this purpose additional carpets can be installed parallel to the two already shown. However, the simulations show that there is a zone directly above and below each carpet where ions will be lost if they start too close to the electrodes. The overall transport efficiency of such an expanded system would therefore be less than unity, assuming random starting points of the ions in the system.

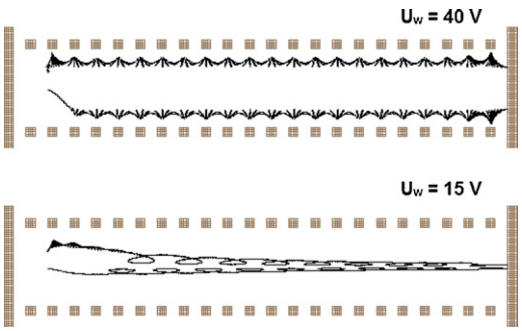

Fig. 10. Ion trajectories calculated with the SIMION code demonstrating the "ion squeezing" variant of ion surfing. Parameter values as given in Table 1 were applied to the carpets and wave amplitudes U_w of 15 V and 40 V were used. A distance of 1.8 mm between the carpets was used. The ions were started on the left side.

4. Summary of ion surfing features

The simulation results obtained in the present work indicate that the ion surfing technique has the potential to overcome some of the shortcomings of present RF ion guiding techniques along surfaces with a relatively simple electrode configuration and RF signal supply.

The main features predicted for ion surfing include

- Fast ion transport. Transport velocities >200 m/s at a helium pressures of 100 mbar at room temperature appear feasible. Classical RF carpets transport techniques would require voltage gradients of more than 100 V/cm to reach similar velocities.
- Low voltage operation. No need for high voltages to transport ions over large distances. High-voltage feedthroughs or isolated segmentation of vacuum chambers are not required.
- Simple circuitry. A small number of different RF signals (minimum 3) is sufficient to supply all RF electrodes.
- Pushing field requirement. For being transported the ions need to be close to the carpet surface. This is not necessary in the case of classical RF carpets; the static axial voltage gradient (drift field) provides transport independent of the ion being close to the carpet surface or not. Multiple layers of ion surfing carpets could eliminate this requirement but would add other constraints.

5. Applications

The ion surfing technique is expected to be useful for all applications where ions need to be transported over a surface for long distances. Two possible applications are discussed.

5.1. Linear gas stoppers

Linear gas stoppers mentioned earlier are used to stop rare isotopes produced in a variety of nuclear reactions at various energies. Ion surfing is most interesting for stopping of high-energy rare isotope beams where a large product of the stopping-length and the gas pressure is required to stop a large fraction of the ions efficiently. RF guiding techniques require relatively low gas pressures, perhaps up to 200 mbar. As a consequence, gas stoppers of up to 2 m in length have been built or are being considered in order to achieve good stopping efficiencies. Given that the rare isotopes often have very short half-lives fast ion extraction from the gas is needed. The strength of guiding electric fields is typically limited to typical values of a few 10 V/cm in order to avoid ion loss or HV breakdowns. A helium pressure of 100 mbar at room temperature and a field strength of 20 V/cm would allow an ion drift velocity of about 40 m/s, much lower than the transport velocities that could be achieved with ion surfing.

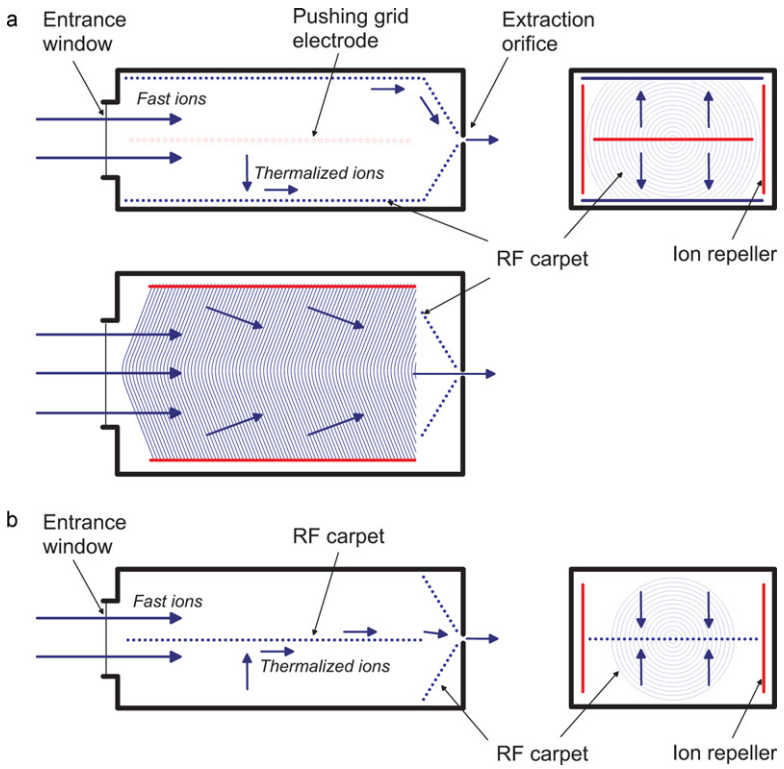

Fig. 11. Schematic representation of ion motion in linear gas stopper systems utilizing the ion-surfing technique with two RF carpets (a) and one central RF carpet (b). See the text for an explanation.

Fig. 11 illustrates a novel concept for linear gas stoppers that employ the ion surfing technique. High voltages are avoided, which means systems of any desired length are possible. However, in contrast to classical RF and DC guiding techniques a pushing field is required. The general devices described here use a rectangularly shaped stopping chamber with an entrance window and an ion extraction orifice at the opposite end. In the configuration depicted in Fig. 11(a) RF carpets are mounted at the top and bottom of the inside of the chamber. In the central plane an electrode grid at positive voltage is installed to provide the pushing field that guides the stopped ions towards the ion-surfing carpet. The carpet electrodes can be shaped such that the ion transport is directed towards the longitudinal axis of the carpet, counteracting outward migration. If needed, additional repeller electrodes at the sides of the carpets can be used to prevent ions from leaving the edges of the RF carpets. In the extraction region an additional RF ion transport system can be used to guide the ions to a central extraction orifice. This small transport system could rely on ion surfing or classical RF transport involving DC voltages or both.

An alternative and somewhat simpler configuration is shown in Fig. 11(b). It uses a single double-sided surfing carpet mounted in the mid plane of the gas stopper. When the appropriate bias is applied the double sided carpet could attract the ions and transport them to the extraction region.

It should be noted that in both configurations the short distance from the RF carpet to the pushing electrode in (a) or the top and bottom chamber walls in (b) may be helpful in efficiently collecting the large number of electrons created during the stopping of the fast ions [26–28]. This may help reduce neutral plasma and space charge effects that cause limitations in the maximum beam rate that gas stoppers can tolerate before experiencing a significant loss in extraction efficiency. The use of a multi-layer carpet system operated in ion-squeezing mode may be even more helpful in this respect and offset the overall reduced efficiency discussed earlier. The shorter electrode distance may allow electrons to be collected more efficiently. Many layers would transport the positive ions, which should help reducing ion losses due to space charge created by the ions themselves. Space charge calculations for such a system are under way.

5.2. Cyclotron gas stopper

A new device for the thermalization of fast ion beams based on the slowing down of ions in a buffer gas contained in a focusing magnetic field is under development [12,29] at MSU. The so-called cyclotron gas stopper takes advantage of the focusing properties of a cyclotron-type magnet that can confine ions in the radial and axial dimensions during the deceleration process. Systems of this kind have been successfully used to stop antiprotons, pions and muons [30] and has been proposed [16] for stopping light ions. Fig. 12 shows the cross section of a schematic cyclotron gas stopper that would incorporate the ion guiding technique

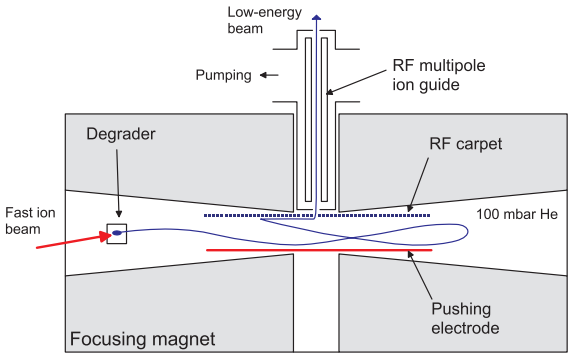

Fig. 12. Schematic cross section of a cyclotron gas stopper employing an ion-surfing RF carpet to guide thermalized ions to the central axis.

for the thermal ions at the end of their range. The cyclotron magnet houses a gas-filled vacuum chamber with a pushing electrode and an ion-surfing RF carpet close to the opposite pole faces. Fast ions are injected tangentially into the system and pass through a solid degrader with a thickness adjusted such that the degraded beam follows an inwards spiraling motion until the ions have reached the end of their range in the gas. The thermalized ions are transported to an extraction orifice on the central axis using the ion-surfing technique. After the ions have left the stopping volume an RF quadrupole ion guide could be used to transport them through a differential pumping system into high vacuum.

Detailed simulations [12] have shown that the ions in such a system stop at radii up to about 50 cm and an RF carpet ion transport system of appropriate size would be required to transport them to the central axis. The use of the ion surfing technique instead of the more classical RF carpet approach would dramatically simplify the RF circuitry and bringing the voltages into the vacuum chamber.

6. Summary and conclusions

A novel ion transport scheme with RF carpets called ion surfing has been developed and investigated with detailed numerical simulations. The simulation results indicate substantial advantages in performance over classical RF transport schemes. The ion-surfing technique can provide a novel simplified scheme for ion transport in linear gas stoppers and promises benefits for a new cyclotron-type gas stopper under development.

Acknowledgments

I would like to thank S. Schwarz, D.J. Morrissey, R. Ringle, G. Pang, and C. Campbell for valuable discussions and acknowledge the support of Michigan State University, the National Science Foundation Grant PHY-0606007, and the US Department of Energy Contract DE-FG02-06ER41413.

References

[1] F. Herfurth, J. Dilling, A. Kellerbauer, G. Bollen, S. Henry, H.-J. Kluge, E. Lamour, D. Lunney, R.B. Moore, C. Scheidenberger, S. Schwarz, G. Sikler, J. Szerypo, Nucl. Instr. Meth. A 469 (254) (2001).
[2] A. Nieminen, J. Huikari, A. Jokinen, J. Äystö, P. Campbell, E. C. A. Cochran and EXOTRAPS collaboration, Nucl. Instr. Meth. A 469 (244) (2001).
[3] S. Schwarz, G. Bollen, D. Lawton, A. Neudert, R. Ringle, P. Schury, T. Sun, Nucl. Instr. Meth. B 204 (2003) 474.
[4] T. Sun, S. Schwarz, G. Bollen, D. Lawton, R. Ringle, P. Schury, Eur. Phys. J. A 25 (S1) (2005) 61.
[5] D. Lunney, C. Bachelet, C. Guenaut, S. Henry, M. Sewtz, Nucl. Instr. Meth A598 (2009) 379.
[6] M. Wada, Y. Ishida, T. Nakamura, Y. Yamazaki, T. Kambara, H. Ohyama, Y. Kanai, T.M. Kojima, Y. Nakai, N. Ohshima, A. Yoshida, T. Kubo, Y. Matsuo, Y. Fukuyama, K. Okada, T. Sonoda, S. Ohtani, K. Noda, H. Kawakami, I. Katayama, Nucl. Instr. Meth. B 204 (2003) 570.
[7] W. Trimble, G. Savard, B. Blank, J.A. Clark, F. Buchinger, T. Cocolios, J.E. Crawford, A. Frankel, J.P. Greene, S. Gulick, J.K.P. Lee, A. Levand, M. Portillo, K.S. Sharma, J.C. Wang, B.J. Zabransky, Z. Zhou, and the S258 Collaboration, Nucl. Phys. A 746 (2004) 415c.
[8] L. Weissman, D.A. Davies, P.A. Lofy, D.J. Morrissey, Nucl. Instr. Meth. A 522 (2004) 212.
[9] L. Weissman, D.A. Davies, P.A. Lofy, D.J. Morrissey, Nucl. Instr. Meth. A 531 (2004) 416.
[10] L. Weissman, D.J. Morrissey, G. Bollen, D.A. Davies, E. Kwan, P.A. Lofy, P. Schury, S. Schwarz, C. Sumithrarachchi, T. Sun, R. Ringle, Nucl. Instr. Meth. A 540 (2005) 245.
[11] S.A. Eliseev, M. Block, A. Chaudhuri, Z. Di, D. Habs, F. Herfurth, H.-J. Kluge, J.B. Neumayr, W.R. Plaß, C. Rauth, P.G. Thirolf, G. Vorobjev, Z. Wang, Nucl. Instr. Meth. B 258 (2007) 479.
[12] G. Bollen, C. Campbell, S. Chouhan, C. Guénaut, D. Lawton, F. Marti, D.J. Morrissey, J. Ottarson, G. Pang, S. Schwarz, A.F. Zeller, P. Zavodszky, Nucl. Instr. Meth. B 266 (2008) 4442.
[13] M. Petrick, W.R. Plaß, K.-H. Behr, A. Brünle, L. Caceres, J. Clark, Z. Di, S. Elisseev, M. Facina, A. Fettouhi, H. Geissel, W. Hüller, M. Huyse, C. Karagiannis, B. Kindler, R. Knöbel, Y. Kudryavtsev, J. Kurcewicz, T. Levant, Yu.A. Litvinov, B. Lommel, M. Maier, D.J. Morrissey, G. Münzenberg, M. Portillo, G. Savard, C. Scheidenberger, P. Van Duppen, H. Weick, M. Winkler, B. Zabransky, Nucl. Instr. Meth. B 266 (2008) 4493.
[14] G. Savard, S. Baker, C. Davids, A.F. Levand, E.F. Moore, R.C. Pardo, R. Vondrasek, B.J. Zabransky, G. Zinkann, Nucl. Instr. Meth. B 266 (2008) 4086.
[15] D.J. Morrissey, G. Bollen, M. Facina, S. Schwarz, Nucl. Instr. Meth. B 266 (2008) 4822.
[16] I. Katayama, M. Wada, H. Kawakami, J. Tanaka, K. Noda, Hyperfine Interact. 115 (1998) 165.
[17] S. Masuda, K. Fujibayashi, K. Ishida, Internationale Staubtagung, Bonn 1970, 30 (Nr 11), Staub-Reinhalt, Luft, 1970, p. 449.
[18] S. Masuda, K. Fujibayashi, K. Ishida, H. Inaba, Elect. Eng. Jpn. 92 (1972) 43.
[19] S. Masuda, M. Washizu, I. Kawabata, IEEE Trans. IAS 24 (1988) 217.
[20] M.D. Lunney, R.B. Moore, Int. J. Mass Spectrom. 190/191 (1999) 153.
[21] E.W. McDaniel, E.W. Mason, The Mobility and Diffusion of Ions in Gases, Wiley, 1973.
[22] S. Schwarz, Int. J. Mass Spectrom 299 (2011) 71–77.
[23] H.G. Dehmelt, Adv. Atom. Mol. Phys. 3 (1967) 53.
[24] SIMION 7.0, Scientific Instrument Services, Inc. http://www.sisweb.com.
[25] K. Giles, Steven D. Pringle, Kenneth R. Worthington, David Little, Jason L. Wildgoose, Robert H. Bateman, Rapid Commun. Mass Spectrom. 18 (2004) 2401.
[26] M. Huyse, M. Facina, Y. Kudryavtsev, P. Van Duppen, and ISOLDE collaboration, Nucl. Instr. Meth. B 187 (2002) 535.
[27] A. Takamine, M. Wada, Y. Ishida, T. Nakamura, K. Okada, Y. Yamazaki1, T. Kambara, Y. Kanai, T.M. Kojima, Y. Nakai, N. Oshima, A. Yoshida, T. Kubo, S. Ohtani, K. Noda, I. Katayama, P. Hostain, V. Varentsov, H. Wollnik, Rev. Sci. Instr. 76 (2005) 103503.
[28] D.J. Morrissey, Eur. Phys. J. Spec. Top. 150 (2006) 365.
[29] G. Bollen, D.J. Morrissey, S. Schwarz, Nucl. Instr. Meth. A 550 (2005) 27.
[30] L.M. Simons, Hyperfine Interact. 81 (1993) 253.